Molecular Catalysis 559 (2024) 114039

Contents lists available at ScienceDirect

Molecular Catalysis

journal homepage: www.journals.elsevier.com/molecular-catalysis

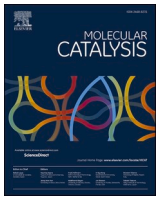

Research Paper

Engineering the enantioselectivity of a novel imine reductase from *Streptomyces viridochromogenes* for the dynamic kinetic reductive amination of cyclic β-ketoester

Xiangyu Zheng [a], Zhe Dou [a,b], Wenqiang Xiang [a], Wen Zhang [a], Ye Ni [a], Guochao Xu [a,*]

[a] Key Laboratory of Industrial Biotechnology, Ministry of Education, School of Biotechnology, Jiangnan University, Wuxi, Jiangsu 214122, China
[b] Collaborative Innovation Center of Yangtze River Delta Region Green Pharmaceuticals, College of Pharmacy, Zhejiang University of Technology, Hangzhou, Zhejiang 310014, China

ARTICLE INFO

Keywords:
Genome mining
Imine reductase
Amine donors
N-substituted β-amino ester
Alanine scanning

ABSTRACT

N-substituted β-amino esters as an important class of chiral amines, are widely used as building blocks in pharmaceuticals. A novel imine reductase *Sv*IRED was identified through gene mining from *Streptomyces viridochromogenes* with high enantioselectivity of > 99 % *ee* (1*R*, 2*S*), 95 % *de* (*cis:trans*), towards 2-oxocyclohexane-1-carboxylate and cyclopropylamine. *Sv*IRED exhibited the highest activity at pH 7.0 and 40 °C. A variety of amine donors could be used by *Sv*IRED and produce chiral *N*-substituted β-amino esters with different enantioselectivity. Employing methylamine (**i**) and pyrrolidine (**n**) as amine donors, *Sv*IRED exhibited reversed enantioselectivity of 23 % *ee* (1*S*, 2*R*) and 79 % *ee* (1*S*, 2*R*) respectively. Through alanine scanning, M183 and H244 were identified with remarkable roles in governing enantioselectivity towards **i** and **n**. Compared with WT *Sv*IRED, the enantioselectivity of M183A was inverted to *ee* value of >99 % (1*R*, 2*S*) and *de* value of >99 % (*cis:trans*) towards **i**, and the enantioselectivity of H244A was inverted to *ee* value of 88 % (1*R*, 2*S*) and *de* value of >99 % (*cis:trans*) towards **n**. Interaction analysis indicated the orientation of ester group was vital for manipulation of enantioselectivity. This study provides novel Imine reductase mutants for enantioselective synthesis of *N*-substituted *β*-amino esters with different amine donors.

1. Introduction

Chiral amines are a kind of important chiral synthons and resolution reagents, which are widely used in the synthesis of natural products, pharmaceutical, pesticides, perfumes and other fine chemicals [1–4]. Conventionally, chiral amines could be synthesized by enamine reduction, amide reduction, imide reduction and asymmetric transfer hydrogenation [5]. However, small organic molecules (chiral diene-borane, chiral phosphoric acid, etc.) or transitional metals (palladium, rhodium, titanium, cobalt, etc.) are usually required as catalysts [6,7], which are unfavorable for industrial application due to harsh reaction conditions, long reaction time, expensive catalysts, environmentally unfriendliness and low optical purity of products. Hence, development of efficient and sustainable synthetic approaches draws increasingly attentions in recent years [8,9].

Biocatalysts have made dramatic advances in the synthesis of optically active fine chemicals especially in the construction of C—N bonds [1]. Primary amines can be achieved by ω-transaminase [10,11], amino acid lyase [12] and amine dehydrogenase [13,14], Recently, considerable progress has been made in amino acid/amine dehydrogenases which utilize ammonia as amine donors and had been evaluated at preparative scale [15]. However, their application scope was limited to the synthesis of primary amines, while the reductive amination of ketones with alkyl amines as amine donors remains a challenge [16]. Advances of imine reductases (IREDs) are conducive to the enantioselectively reductive amination of ketones with secondary amines. Compared with other C—N constructing enzymes, IREDs are more advantageous in the synthesis of a variety of primary, secondary, and even tertiary amine products for the preparation of various APIs and scaffolds [17–20]. Particularly, the newly discovered reductive aminase (RedAms) [21], a subclass of IREDs, can not only catalyze the reduction of imines, but also catalyze the formation of imine intermediates between prochiral ketones or aldehydes and amines, and the subsequent asymmetric reduction into chiral amine with high enantioselective and

* Corresponding author.
E-mail address: guochaoxu@jiangnan.edu.cn (G. Xu).

https://doi.org/10.1016/j.mcat.2024.114039
Received 24 January 2024; Received in revised form 5 March 2024; Accepted 11 March 2024
Available online 23 March 2024

100 % theoretical conversion, in addition to high atomic economy and low environmental factor [1].

Since the first discovery in 2017, RedAms have gradually been applied in the synthesis of various drugs or drug intermediates such as *N*-substituted-α/β/δ-amino esters and γ-lactam [17,22]. The chiral intermediate of Resagiline can be achieved by Q240A of *Asp*RedAm with turnover number of 32,000 and space-time yield of 3.73 $g{\cdot}L^{-1}{\cdot}d^{-1}$. A variety of amine donors can be utilized to catalyze the asymmetric reductive amination of a series of prochiral ketones, and the conversion ratios can surpass 90 % even at molar ratio of 1:1 between ketone and amine donor [21]. A panel of IREDs for the synthesis of azacycloalkylamines by Gao et al. and metagenomic library by Turner et al. were established [23,17], which demonstrated that IREDs are capable of synthesizing diverse target blocks and scaffolds, further highlighting the huge potential application of IREDs. Moreover, IREDs have been applied in the industrially biocatalytic synthesis of chiral amines. Pfizer reported that *Sp*RedAms catalyzed the direct reductive amination of ketones with methylamine, and successfully implemented in the commercial preparation of JAK1 inhibitor Abcittinib intermediate employing evolved mutant *Sp*RedAm-R3-V6 [16], with a significantly increased space-time yield of 60 $g{\cdot}L^{-1}{\cdot}d^{-1}$. In addition, GSK achieved commercial manufacturing of LSD1 inhibitor GSK2879552 through reductive amination of ketones and amines [24]. Furthermore, different amine donors can also be used in constructing different C—N bonds to enrich the building blocks of pharmaceuticals. In recent years, many researchers have been increasingly interested in expanding the scope of amine donors involved in the reductive amination process, from small and simple amines to bulky and challenging amines [25–27]. Zheng et al. had successfully engineered the amine donors' scope of *Pc*-IRED [28]. Employing *Pc*-IRED-M_3, cinacalcet was successfully prepared with high enantioselectivity of >99 % (*R*) and yield of 84.7 %. Although different amine donors have been well implemented in the reductive amination reactions, the underlying molecular mechanism of amine donors influencing enantioselectivity remains to be clarified.

In this study, cyclic *β*-ketoesters, ethyl 2-oxocyclohexane-1-carboxylate, was selected as a model amine receptor, which could be asymmetrically reduced into *N*-substituted *β*-amino esters. Optically active *N*-substituted *β*-amino esters are important chiral building blocks for many antifungal drugs and active pharmaceutical ingredients [29–30]. Cyclic *β*-ketoesters can be spontaneously racemized and used to develop dynamic kinetic reductive amination (DKRA) reactions featuring 100 % theoretical yield [31]. However, only a few enzymes had been reported with desired selectivity and activity towards cyclic *β*-ketoesters. pIR361 was identified from the metagenomic IRED library and exhibited *ee* value of >99 % (1*R*, 2*S*), while the *de* value was only 62 % (*cis:trans*), which was unfavorable for the application in the synthesis of *N*-substituted *β*-amino esters [17].

Herein, a novel IRED was identified from *Streptomyces viridochromogenes* by gene mining and designated as *Sv*IRED. *Sv*IRED displayed high enantioselectivity and diastereoselectivity with >99 % *ee* (1*R*, 2*S*) and 98 % *de* (*cis:trans*) in the synthesis of cyclic *N*-substituted *β*-amino ester with cyclopropylamine as amine donor. Various amine donors could be accepted by *Sv*IRED for constructing of diverse chiral C—N units through dynamic kinetic reductive amination of ethyl 2-oxocyclohexane-1-carboxylate. Influence of different amine donors on catalytic activity and stereoselectivity were explored through alanine scanning and saturation mutagenesis. Interaction analysis was performed to elucidate the underlying molecular mechanism on enantioselectivity regulation by amine donors. This study provides a novel and highly selective biocatalysts for the enantioselective and sustainable synthesis of chiral cyclic *N*-substituted *β*-amino esters, and provides useful guidance for engineering the amine donors' scope of homologous IREDs.

2. Material and method

2.1. Materials

The substrate ethyl 2-oxocyclohexane-1-carboxylate and all the amine donors used in this study were purchased from Sigma-Aldrich (Stockholm, Sweden), Aladdin (Beijing, China) or Macklin (Shanghai, China). Cofactors $NADP^+$/NADPH were purchased from Bontac Bioengineering Co. ltd (Shenzhen, China). All the PCR reagents and enzymes were purchased from TaKaRa Biotechnology Co. (Dalian, China), Primers for site-directed mutagenesis were synthesized by Talen-bio Biological Technology Co. (Shanghai, China). Expression vector pET28a and recombinant strain *E. coli* BL21(DE3) were previously constructed and stored in our lab. Glucose dehydrogenase (BmGDH) derived from *Bacillus megatherium* were stored in our lab for cofactor regeneration.

2.2. Heterogenous expression of Imine reductase

Recombinant plasmids harboring genes coding for IREDs were chemically transformed into competent cells of *E. coli* BL21(DE3), followed by spread on LB plate supplemented with 50 $\mu g{\cdot}mL^{-1}$ kanamycin and cultivated at 37 °C for 12 h. Subsequently, the positive single colonies were picked up from the plate and transferred into a flask with 40 mL LB liquid medium containing 50 $\mu g{\cdot}mL^{-1}$ kanamycin and cultivated at 37 °C and 120 rpm for 6–8 h as the seed. Furthermore, the culture was inoculated at dosage of 1 ‰ (v/v) into a flask with 80 mL fresh LB liquid medium containing 50 $\mu g{\cdot}mL^{-1}$ kanamycin and further cultivated at 37 °C and 120 rpm. until the OD_{600} reached 0.6–0.8. Then, isopropyl β-D-1-thiogalactopyranoside (IPTG) was added to the final concentration of 0.2 mM for inducing the expression of IREDs at 16 °C and 180 rpm for 16 h. Cells were harvested by centrifuge at 4 °C at 8000 rpm for 5 min and suspended in 10 mL sodium phosphate buffer (pH 7.0, 0.1 M), and subsequently lysed by ultrasonication (250 W, work 2 s, intermittent 3 s for 15 min) in ice-water bath. After centrifuge at 8000 rpm at 4 °C for 30 min, the supernatant was obtained as the crude enzyme solution of recombinant IREDs. Crude enzyme solution was further lyophilized to obtain the dry powder of enzyme and stored at 4 °C for further analysis.

2.3. General method for activity assay

Activity of IREDs was spectrophotometrically determined by monitoring the absorbance changes of NADPH at OD_{340}. The general activity assay was conducted in a 200-μL reaction mixture constituted of 10 μL 3-phenylpropanal (5 mM), 10 μL propargyl (10 mM), 10 μL NADPH (1 mM), 10 μL enzyme solution pre-diluted to appropriate concentration, and 160 μL PBS buffer (pH 7.0, 100 mM). Reaction was maintained at 30 °C, and the OD_{340} was monitored for 3 min. One unit (U) of enzyme activity was defined as the amount of enzyme required for the reduction of 1 μmol NADPH. The concentration of enzyme was determined by Bradford method using bovine serum albumin as the standard protein.

2.4. Purification of SvIRED and GDH

Cells were resuspended in 15 mL binding solution buffer A (20 mM imidazole, 500 mM NaCl, 25 mM Tris–HCl, 10 % glycerol, pH 7.4) per one gram of recombinant cells, and disrupted by high pressure homogenizer for 3 times under the condition of 0 °C and 800 bar. Then, lysate was centrifuged at 4 °C and 8000 rpm for 30 min to remove the cell debris. The supernatant was used as the crude enzyme solution for purification. Enzyme solution was filtrated through a 0.22 μm filter, and loaded on a 1.5 mL Ni-NTA Sefinose column (Sangon Biotech Co., Ltd.). The crude enzyme was gradient eluted with different concentrations of imidazole ranging from 10 mM to 500 mM. All the elution fractions were collected and analyzed by SDS-PAGE. The corresponding bands with high purity of *Sv*IRED and GDH were desalted and concentrated.

Concentrations of purified *Sv*IRED and GDH were measured by Nanodrop 2000c (Thermo Electron Co., Ltd.), and then quickly frozen in liquid N_2 and stored at –80 °C for enzyme characterization.

2.5. Enzyme characterization of purified SvIRED

Influence of pH on the activity of purified *Sv*IRED was investigated in different buffers using the general activity assay method at 30 °C, including sodium citrate buffer (pH 4.0–6.0, 100 mM), sodium phosphate buffer (pH 6.0–8.0, 100 mM), Tris–HCl buffer (pH 8.0–9.0, 100 mM). The highest activity was defined as 100 %. All activity assays were performed for at least three times.

Effect of temperature on the activity of purified *Sv*IRED was evaluated at different temperatures ranging from 20 °C to 50 °C in PBS buffer (pH 7.0, 100 mM) employing the general activity assay method. The highest activity was regarded as 100 %. The purified *Sv*IRED was incubated at 30 °C, 40 °C, 50 °C and the residual activities were monitored over time to calculate its thermostability. The initial activity was defined as 100 %. All activity assays were conducted in triplicate.

Effect of metal ions including Na^+, Zn^{2+}, Co^{2+}, Cu^{2+}, Ni^{2+}, Fe^{3+}, Al^{3+}, Fe^{2+}, Mn^{2+}, Ca^{2+} and EDTA on the activity of purified *Sv*IRED was explored. Tris–HCl buffer (pH 7.0, 20 mM) instead of PBS was adopted to eliminate the interference of Na^+. Metal ions with a final concentration of 1 mM were incubated with an appropriate concentration of purified *Sv*IRED at 30 °C for 1 h to determine the residual activity employing the general method for activity assay. Control experimental was carried out by incubation equal volume of deionized water, and its activity was defined as 100 %. All assays were conducted for at least three times

2.6. Site-directed mutagenesis of SvIRED

Site-directed mutagenesis was performed using recombinant plasmid containing *Sv*IRED gene as template with a 20 μL PCR reaction system (**Table S1**) and three-step PCR amplification procedure (**Table S2**). The PCR products were digested by *Dpn*I (Takara, Shanghai) and transformed into *E. coli.* BL21 (DE3) cells. The mutation sequences were verified by DNA sequencing. The positive single colony was transferred, and expression of *Sv*IRED mutant genes was induced via IPTG at a final concentration of 0.2 mM. The crude enzyme solution of *Sv*IRED mutants were prepared as above mentioned, and the conversion ratio and selectivity of *Sv*IRED mutants were detected by GC analysis. The primers used in this work are shown in **Table S3.**

2.7. General procedure for the preparation of standards by chemical reductive amination

General preparation process: In a 50 mL conical flask with 10 mL 1,2-dichloroethane as the reaction solvent, 2 mM ethyl 2-oxocyclohexane-1-carboxylate (**1**), 2 mM amine donor, 3 mM $NaBH(OAc)_3$ were added, respectively. Finally, an appropriate amount of trifluoroacetic acid was added to increase the reaction rate. The reaction mixture was stirred overnight at 16 °C. Then the reaction was quenched by adding 1.0 M aqueous Na_2CO_3 and extracted with ethyl acetate. The organic phase was dried over anhydrous Na_2SO_4, and organic solvent was removed under reduced pressure to afford the desired product. The corresponding hydrochloride was obtained by addition of 2.0 M HCl in diethyl ether and drying under vacuum.

2.8. Determination of conversion ratio, diastereoselectivity and enantioselectivity

A typical 500-μL reaction mixture contained 10 mM ethyl 2-oxocyclohexane-1-carboxylate (**1**), 20 mM amine donor, 4 mg·mL^{-1} purified *Sv*IRED, 6 U·mL^{-1} glucose dehydrogenase (GDH), 0.5 mM $NADP^+$, 50 mM glucose, 5 % (v/v) ethanol in sodium phosphate buffer (100 mM, pH 7.0). The reaction mixture was incubated at 30 °C with shaking at 180 rpm for 12 h and quenched by the addition of 100 μL of 1.0 M sodium carbonate and extracted with 500 μL methyl tert-butyl ether. The organic phase was dried over anhydrous Na_2SO_4 and monitored by GC equipped with CP-ChiraSil-DeX CB column to determine the conversion ratio and enantioselectivity. Chiral GC analysis: injector temperature: 280 °C, detector temperature: 280 °C, column temperature program: holding at 80 °C for 2 min, increase to 150 °C at increment of 5 °C/min and holding at 150 °C for 2 min, further increase 180 °C at increment of 10 °C/min and holding at 180 °C for 10 min. Retention times of (1*R*, 2*S*), (1S, 2*R*), (1*S*, 2*S*), and (1*R*, 2*R*) were 16.1, 16.3, 16.5, and 16.8 min respectively. Diastereoselectivity (diastereomeric excess, *de*) and enantioselectivity (enantiomeric excess, *ee*) values were determined according to the following equations.

$$de\ (\%) = \frac{cis - trans}{cis + trans} \times\ 100 \tag{1}$$

$$ee\ (\%) = \frac{(1R,2S) - (1S,2R)}{(1R,2S) + (1S,2R)} \times\ 100 \tag{2}$$

2.9. Determination of kinetic parameters

Kinetic parameters of wild type and variant D246A were determined by measuring initial rates of consumption of substrate 1 by GC. Reaction mixture contained 0.5–20 mM of ethyl 2-oxocyclohexane-1-carboxylate (**1**), 20 mM cyclopropylamine (**a**) or methyl amine (**i**), 6 U·mL^{-1} glucose dehydrogenase (GDH), 0.5 mM $NADP^+$, 50 mM glucose, 5 % (v/v) ethanol and purified enzyme in a total volume of 500 μL in sodium phosphate buffer (100 mM, pH 7.0). Kinetic parameters were determined through non-linear regression based on Michaelis-Menten kinetics using OriginPro2022 software.

2.10. Molecular docking and interaction analysis

Structure model of *Sv*IRED was built by AlphaFold 2 and verified by SAVES. Cofactor NADPH and substrate were docked into the active center of *Sv*IRED using the CDOCKER module of Discovery studio 4.5. Residues D176, T99, and W184 were defined as the combined pocket cavity. Interaction analysis was implemented using Discovery studio, and analysis result was visualized employing Pymol.

2.11. Preparative scale reductive amination

For preparative scale reductive amination, a typical 20 mL reaction mixture contained 50 mM ethyl 2-oxocyclohexane-1-carboxylate, 100 mM amine donors (a, i, or, n), cell-free extracts of IREDs (200 mg), 15 U·mL^{-1} glucose dehydrogenase (GDH), 0.5 mM $NADP^+$, 150 mM glucose, 5 % (v/v) DMSO. The reaction volume was made up to 20 mL with sodium phosphate buffer (100 mM, pH 7.0). 2 M NaOH was titrated into the reaction mixture to maintain the pH at 7.0 during reaction. Then the reaction was quenched by adding 2.12 g Na_2CO_3 and extracted with equal volume ethyl acetate for three times. The organic phase was combined and dried over anhydrous Na_2SO_4, and organic solvent was removed under reduced pressure to afford the desired product. The corresponding hydrochloride form of products was obtained by addition of 2.0 M HCl in diethyl ether and drying under vacuum. Appropriate amount of product was dissolved in methanol-d_4 for NMR verification.

3. Results and discussion

3.1. Identification of IREDs for reductive amination of ethyl 2-oxocyclohexane-1-carboxylate with cyclopropylamine

Chemical synthetic methods for cyclic *N*-substituted β-amino ester mainly use (*S*)-phenethylamine as chiral auxiliary reagents, with the

highest selectivity of 84 % *de* under the optimal conditions [32]. Hence, tedious recrystallization was required to obtain optically pure enantiomers. Recombinant IRED pIR361 was reported with activity in the synthesis of cyclic *N*-substituted *β*-amino ester by dynamic kinetic resolution of ethyl 2-oxocyclohexane-1-carboxylate with cyclopropylamine with *ee* value of 99 % (1*R*, 2*S*) while *de* value of merely 62 % (*cis:trans*). To the best of our knowledge, this is the only enzyme reported with activity towards ethyl 2-oxocyclohexane-1-carboxylate. To obtain a novel IRED with high stereoselectivity for preparation of cyclic *N*-substituted β-amino esters, a total of six putative IREDs with 30–80 % identity in sequence with pIR361 were selected from NCBI database for heterogeneously expressed in *E. coli* BL21(DE3), and were evaluated in the reductive amination of ethyl 2-oxocyclohexane-1-carboxylate and cyclopropylamine.

All the six recombinant IREDs was successfully expressed in *E. coli* BL21(DE3) according to the SDS-PAGE analysis **(Fig. S1)**, and they were subsequently evaluated in the reductive amination of ethyl 2-oxocyclohexane-1-carboxylate (Table 1). Conversion analysis revealed that all IREDs could catalyze the reductive amination of ethyl 2-oxocyclohexane-1-carboxylate with cyclopropylamine as amine donor, however, with different catalytic activity, enantioselectivity and diastereoselectivity. *Sv*IRED from *Streptomyces viridochromogenes* exhibited the highest conversion ratio of >99 %, and relatively high stereoselectivity of 95 % *de* (*cis:trans*) and >99 % *ee* (1*R*, 2*S*). Although *Ad*IRED from *Ajellomyces dermatitidis* displayed the high *ee* value of >99 % (1*R*, 2*S*), its catalytic activity was extremely low with merely 3 % conversion under same reaction conditions. Moreover, the diastereoselectivity of *Ad*IRED was also low with *de* value of 56 % (*trans:cis*). *Sc*IRED from *Streptomyces cyaneofuscatus* and *Mc*RA from *Micromonospora chinaurantiaca* displayed inverted enantioselectivity compared with pIR361 (Table 1). Considering the highest activity and selectivity of *Sv*IRED, it was selected for further characterization and study.

3.2. Enzyme characterization of SvIRED

Recombinant *Sv*IRED was purified using nickel-affinity chromatography. SDS-PAGE analysis showed that *Sv*IRED was purified to electrophoretic purity. And the purified bands migrated at around 30 kDa, which was matched with its theoretical molecular weight **(Fig. S2)**. Specific activity of purified *Sv*IRED was 0.94 U•mg^{-1} using 3-phenylpropanal and propargyl as substrates, higher than 0.14 U•mg^{-1} of crude enzyme, indicating a purification-fold of 6.7.

Subsequently, effects of pH and temperature on the catalytic activity of purified *Sv*IRED were explored. Characterization of pH- and temperature-profiles was conducive to the optimization of biocatalytic reaction. Various buffers with different pH values were selected to test the relative activity of *Sv*IRED. As shown in the Fig. 1**A**, the optimal pH of *Sv*IRED was 7.0, with the highest activity of 0.94 U•mg^{-1}. The relative activity at pH 6.0 and pH 8.0 was 69.3 % and 50.0 % of highest activity, respectively. When the pH was lower than 6.0 or higher than 8.0, the catalytic activity decreased significantly. As illustrated in Fig. 1**B**, the relative activity of *Sv*IRED at temperature ranging from 20 °C to 55 °C were also detected. The activity increased gradually between 20 °C and 40 °C, and the highest catalytic activity was monitored at 40 °C, with specific activity of 1.65 U•mg^{-1}. Further increasing the temperature to 50 °C, the activity of *Sv*IRED decreased rapidly, which was just 50 % of the highest activity at 40 °C.

Thermostability of *Sv*IRED was investigated at 30 °C, 40 °C, and 50 °C. The half-life of *Sv*IRED at 30 °C was calculated to be 38.5 h (Fig. 1**C**), while its half-lives at 40 °C and 50 °C were 2.0 h and 2.3 min. respectively. All above indicated *Sv*IRED is a mesophilic enzyme with higher stability at 30 °C than 40 °C and 50 °C. As far as we know, thermostability of homologous IREDs has not been reported. Directed evolution of its thermostability and identification of thermostable IREDs is of special interests and ongoing in our lab. Above all, investigation on the pH and thermostability of *Sv*IRED guided us to carry out the subsequent reductive amination reactions under the optimal condition of PBS 7.0 and 30 °C.

Influence of metal ions on the activity of *Sv*IRED was explored by incubating purified *Sv*IRED with diverse metal ions and EDTA. As shown in Fig. 1**D**, metal ions including Zn^{2+}, Co^{2+}, Cu^{2+}, Ni^{2+}, Fe^{2+} has obvious adverse effect on the activities of *Sv*IRED, with the relativity activities of 50.0 %, 81.2 %, 39.0 %,73.8 % respectively. While the relative activities of *Sv*IRED were increased to 121 % and 110 % under assistance of Mn^{2+} and Ca^{2+}. Moreover, addition of EDTA resulted in a slightly decreased relativity activity to 92.8 %. All above indicated that although the activity of *Sv*IRED is not highly dependent on metal ions while Mn^{2+} is favorable for the activity of *Sv*IRED through stabilization of its spatial conformation.

Kinetic parameters of WT toward ethyl 2-oxocyclohexane-1-carboxylate (**1**) and different amine donors including cyclopropylamine (**a**) and methyl amine (**i**) (**Table S4**). The K_M and k_{cat} values of WT toward cyclopropylamine (**a**) were 5.49 mM and 0.78 min^{-1}, resulting in k_{cat}/K_M value of 140 min^{-1}·M^{-1}. With regard to methyl amine (**i**) as amine donor, the K_M and k_{cat} values of WT were 12.22 mM and 0.002 min^{-1}, with k_{cat}/K_M value calculated to be 6.4 min^{-1}·M^{-1}. The higher k_{cat}/K_M value toward cyclopropylamine (**a**) than methyl amine (**i**) indicated cyclopropylamine is more favorable for donating amine group toward ethyl 2-oxocyclohexane-1-carboxylate (**1**).

Table 1
Result of conversion and enantioselectivity toward ethyl 2-oxocyclohexane-1-carboxylate (**1**) and cyclopropylamine (**a**).

Enzyme	Microorganism	Identity (%)	Conv. (%)	*de* (*cis:trans*) (%)	*ee* (1*R*, 2*S*) (%)
pIR361	*Streptomyces bluensis*	100	>99	62	>99
*Ad*IRED	*Ajellomyces dermatitidis*	33.8	3 ± 1	–56	>99
*My*IRED	*Myxococcus* sp. AM401	33.9	62±2	80	57
*Sv*IRED	*Streptomyces viridochromogenes*	73.3	>99	95	>99
*Cf*IRED	*Cystobacter ferrugineus*	33.4	18±1	43	50
*Sc*IRED	*Streptomyces cyaneofuscatus*	49.8	48±1	>99	–99
*Mc*IRED	*Micromonospora chinaurantiaca*	41.3	36±1	44	–33

3.3. Dynamic kinetic reductive amination of ethyl 2-oxocyclohexane-1-carboxylate (1) towards different amine donors

To explore preference of *Sv*IRED towards amine donors, different amine donors (**a**-**n**) with diverse substituents including primary amines with small hindrance and secondary amines even large hindrance primary amines were selected to explore the influence of amine donors in the dynamic kinetic reductive amination (DKRA). As shown Table 2, amine donors displayed significant influence not only on conversion ratios, but also on enantioselectivity of *Sv*IRED catalyzed DKRA reactions.

According to the proposed catalytic mechanism of *At*RedAm [33], the nitrogen atom of amines may interact with N93, and the allyl group of amines is bound in the pockets formed by the side chains of L96 and I123. Moreover, π-system interactions were found between the main amido-carbonyl and amine groups of these residues. Both hydrogen bonding interaction between π-system and backbone residues are critical [34,35]. These sites were found to be conserved residues of IREDs from multiple sequence alignment (**Fig. S3**). Hence, small amine donors with *π*-characteristics such as cyclopropylamine (**a**), propargyl (**b**), and allylamine (**c**) are easy to be accepted, and *Sv*IRED also showed conversion ratios of >99 %, 98 %, and 92 %, respectively. While isopropylamine (**h**) are hard to be acceptable by *Sv*IRED with conversion

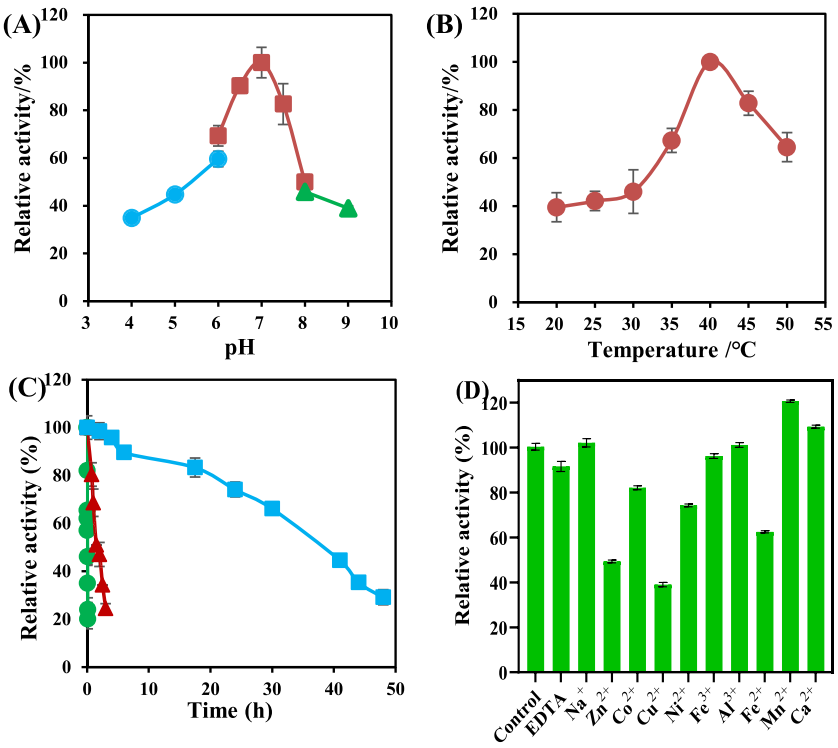

Fig. 1. Effects of pH, temperature and metal ions on the activity of *Sv*IRED.
(A) pH-profile, (●): sodium citrate buffer, (●): sodium phosphate buffer, (●): Tris–HCl buffer. (B) Temperature-profile. (C) Thermostability, (●): 30 °C, (●): 40 °C, (●): 50 °C. (D) Metal ions.

Table 2
Influence of amine donors on the DKRA reactions of *Sv*IRED.

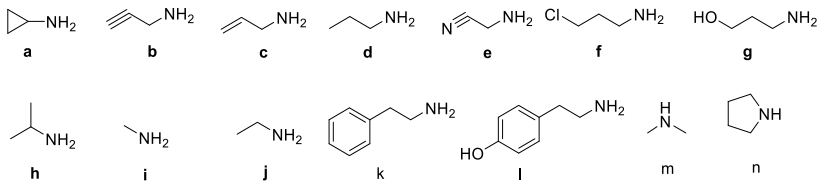

Amine donor[a]	Conv. (%)	$de_{(cis:trans)}$ (%)	*ee* (%)	Amine donor	Conv. (%)	$de_{(cis:trans)}$ (%)	*ee* (%)
a	>99	95	$>99^{(1R,2S)}$	**h**	3 ± 1	>99	$>99^{(1R,2S)}$
b	98±1	>99	$79^{(1R,2S)}$	**i**	85±1	>99	$23^{(1S,2R)}$
c	92±1	81	$71^{(1R,2S)}$	**j**	48±1	>99	$78^{(1R,2S)}$
d	82±1	92	$84^{(1R,2S)}$	**k**	*n. d.*	*n. d.*	*n. d.*
e	42±2	61	$49^{(1R,2S)}$	**l**	*n. d.*	*n. d.*	*n. d.*
f	17±1	>99	$>99^{(1R,2S)}$	**m**	*n. d.*	*n. d.*	*n. d.*
g	*n. d.*[b]	*n. d.*	*n. d.*	**n**	19±11	>99	$79^{(1S,2R)}$

Reaction conditions: A total of 500 μL reaction mixture containing 10 mM **1**, 20 mM different amine donor, 4 mg·mL^{-1} purified *Sv*IRED, 6 U·mL^{-1} purified GDH, 0.5 mM $NADP^+$, 50 mM glucose, 5 % (v/v) ethanol in PBS buffer (100 mM, pH 7.0) was shaken at 200 rpm and 30 °C for 12 h. Conversion ratios, *de* and *ee* values were determined by chiral GC.
[a] : Two equivalents of amine donors were used.
[b] *n. d.*: no activity was determined.

ratio of merely 3 %, which is consistent with our experimental results. Besides, it was likely that the amines (**k, l**) with large hindrance encountered greater barriers to entry into the active center to form imine intermediates, resulting in the loss of catalytic activity. Interestingly, it was found that the catalytic activity of *Sv*IRED was significantly decreased or even deactivated when electron-withdrawing groups such as -Cl/-OH groups were added to propylamine. However, excellent diastereoselectivity and enantioselectivity with >99 % *de* and >99 % *ee* were detected toward 3-chloropropan-1-amine (**f**) despite the low conversion ratio of 17 %. Only *cis*-products were produced with amine

donors of **b, f, h-j**, and **n**. More importantly, the enantioselectivity was inverted from (1*R*, 2*S*) to (1*S*, 2*R*) towards smaller amines including methyl amine (**i**) and pyrrolidine (**n**), with *ee* values of 23 % (1*S*, 2*R*) and 79 % (1*S*, 2*R*), respectively. The discovery of amine donors influencing the diastereoselectivity and enantioselectivity on *Sv*IRED is of interest to elucidate the catalytic mechanism of Imine reductase.

3.4. Site-directed mutagenesis of the residues in substrate binding pocket of SvIRED

To gain deep insight into factors contributing to switch of stereoselectivity by amine donor **i** and **n,** the structure model of *Sv*IRED was predicted using AlphaFold2. Substrate (corresponding imine forms of different amine donors) and NADPH were docked into the active center of *Sv*IRED. Based on the molecular docking analysis, the ester chain of substrate exhibited opposite orientations (Fig. 2), which could potentially account for the reversal stereoselectivity. Furthermore, the distances between the prochiral C atom of the carbonyl group of substrate and C4 atom of NADPH was 4.2 Å with the cyclopropylamine(**a**) which was longer than 4.1 Å and 4.0 Å with **i** and **n** respectively (Fig. 2). It further provided evidence for the influence of conversion ratios by different amine donors, which was mainly attributed to the structural characteristic of amine donors.

In order to understand the mechanism of selectivity toward different amine donors of *Sv*IRED, residues lining the substrate binding pocket in 6 Å of *Sv*IRED were selected for site-directed mutagenesis. As illustrated in Fig. 3**A**, residues including D246, M125, M19, L179, L180, I127, V137, M183, P128, I124, I218, M214, V217, H244, D238, and V243 were submitted for alanine scanning. Subsequently, the conversion ratios and selectivity of the mutants towards cyclopropylamine (**a**), methylamine (**i**) and pyrrolidine (**n**) were monitored. As shown in Table 3, all the mutants retained reductive amination activity towards **a** (13.1–203.3 %), **i** (11.6–110.0 %), and **n** (9.7–442.1 %). Especially, the relative activities of D246A were significantly increased to 203.3 %, 110.0 %, and 442.1 %, ranking the most efficient enzymes. For cyclopropylamine (**a**), the relative activities of M19A, M125A, D246A, L179A, and I124A were higher than WT, while for methylamine (**i**), the relative activities of D246A and I124A were higher than WT. With regard to pyrrolidine (**n**), M19A, M125A, D246A, I124A, P128A, M183A, I218A, H244A, and D238A were more efficient than WT. All above proved that the amine donors' scope of *Sv*IRED could be manipulated.

Furthermore, the influence of mutants on the diastereoselectivity and enantioselectivity of *Sv*IRED toward different amine donors were analyzed as shown in Fig. 3. For cyclopropylamine (**a**), there is no significant influence on the selectivity of mutants. **(**Fig. 3**B)**. Mutant L180A displayed excellent selectivity with *ee* value of >99.9 % (1*R*, 2*S*) and *de* value of >99.9 % (*cis:trans*). While mutants M19A, M125A, D246A and L179A retained similar *ee* value of >99 % as WT. No selective inversion was observed when **a** was used as amine donor, while mutants H244A, D238A, V243A displayed significantly decreased stereoselectivity with *ee* values of 53.4 %, 48.7 %, 45.7 % respectively, suggesting these residues may play a key role in the regulation of enantioselectivity. In the asymmetric reductive amination with **i**, mutants showed drastically different enantioselectivity, besides *de* values of >99.9 % (*cis:trans*) (Fig. 3**C**). Compared with WT, only mutant M214A showed increased enantioselectivity with *ee* values of 34.3 % (1*S*, 2*R*). Mutants M125A, D246A, I218A, D238A, I127A, P128A, H244A, V243A, L180A, and M183A exhibited reversed enantioselectivity. Most importantly, mutant M183A showed a remarkable changed enantioselectivity, with *ee* value switched from 23 % (1*S*, 2*R*) to >99.9 % (1*R*, 2*S*), demonstrating the pivotal role of M183 in manipulating the enantioselectivity of **i**. regarding to amine donor **n**, only mutants M19A, M125A, and I218A exhibited increased enantioselectivity with *ee* value of 93.9 % (1*S*, 2*R*), 86.1 % (1*S*, 2*R*), and 82.1 % (1*S*, 2*R*) respectively (Fig. 3**D**). Interestingly, enantioselectivity of V217A, L180A, V243A, and H244A were inverted into (1*R*, 2*S*) from (1*S*, 2*R*). H244A displayed the highest (1*R*, 2*S*)-selectivity of 88.4 % *ee*. All above proved that the enantioselectivity and diastereoselectivity of *Sv*IRED toward different amine donors could be facilely manipulated.

Preparative scale reactions were performed to demonstrate the utility of L180A, M183A and H244A with high selectivity towards cyclopropylamine (**a**), methylamine (**i**) and pyrrolidine (**n**) in the synthesis of *N*-substituted *β*-amino esters. Ethyl 2-oxocyclohexane-1-carboxylate with cyclopropylamine (**a**) could be completely reductive aminated with isolation yields of 92.1 %, 86.5 % and 70.3 % within 48 h by L180A, M183A and H244A respectively (**Table S5**). All isolated products were verified by ^{1}H NMR and ^{13}C NMR as shown in **Figs. S9-S14**.

3.5. Interaction analysis of SvIRED and mutants towards methylamine (i) and pyrrolidine (n)

Mutation of residues surrounding substrate into alanine could facilitate the formation of beneficial substrate cavity, promoting the accommodation of substrate in a favorable conformation and produce product with desired configuration. Good performance of M183A and H244A encouraged us to perform molecular docking analysis of **1** with **i** and **n** to disclose the underlying molecular mechanism. D176 had strong attractive interaction with nitrogen of substrate imide, which played an important role in catalytic process [33]. Nevertheless, tremendous changes were observed between WT and M183A or H244A according to the docking results. As for **i**, alkyl interaction was observed between cyclic ring of substrate and the side chains of L180 and M183 as shown in Fig. 4**A**. M183 was adjacent to L180, which may lead to a serious steric hindrance effect, causing the orientation of ester chain of substrate to deviate from the direction of M183. Compared with WT, mutation of Met into Ala resulted in less attractive interaction towards substrate, which was consistent with the lower relative activity of 88 %. Moreover, steric hindrance was drastically reduced by alanine mutation, resulted in a strong alkyl interaction between side chain of L180 and ester group of substrate. Hence, the orientation of ester chain was completely reversed (Fig. 4**B**), making M183A preferable to produce (1*R*,2*S*)-enantiomer. Regarding to amine donor of **n**, the substrate was located in the active center of WT in an outward orientation with the ester chain group

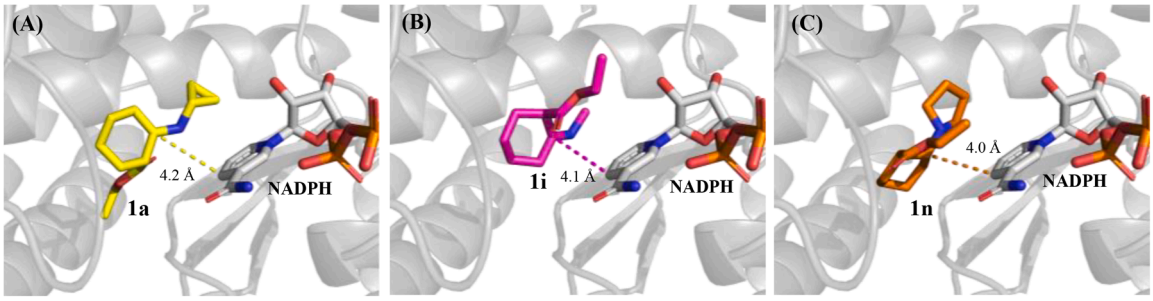

Fig. 2. Molecular docking analysis of ethyl 2-oxocyclohexane-1-carboxylate with cyclopropylamine **a** (A), methyl amine **i** (B), and pyrrolidine **n** (C).

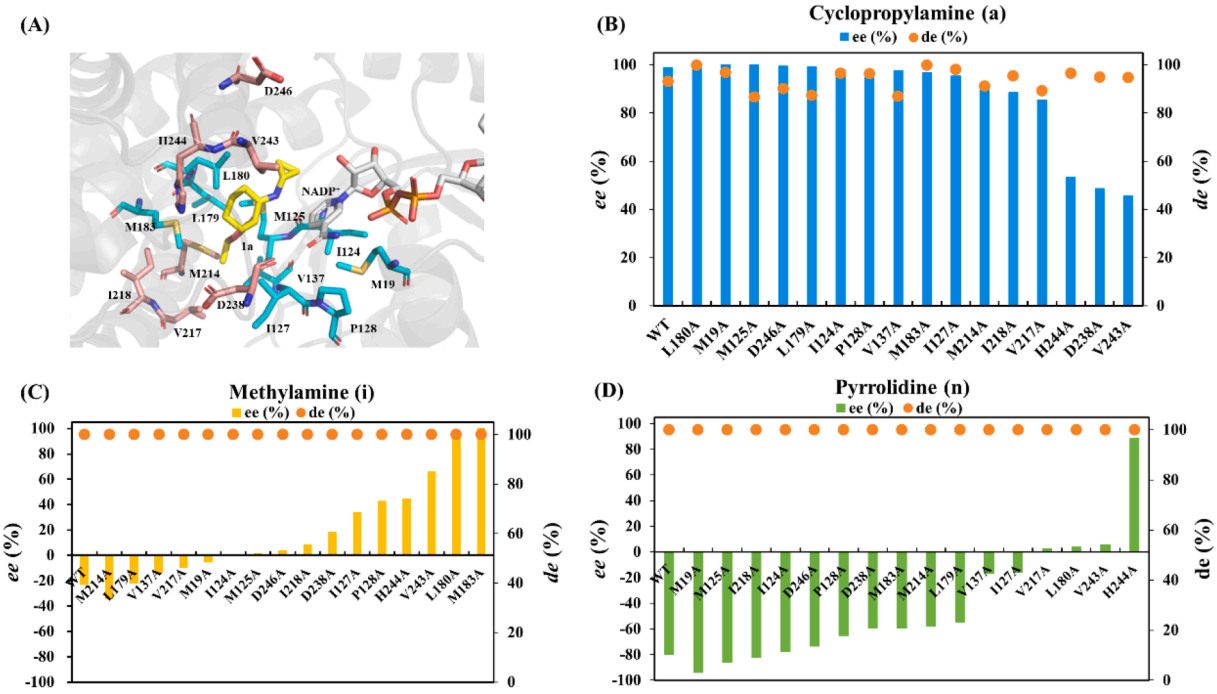

Fig. 3. Residues in the substrate binding pocket of *Sv*IRED and alanine scanning results towards **a, i, n**. (A) Residues within 6 Å of substrate; (B) *ee* and *de* values of alanine scanning mutants toward **a**, (C) *ee* and *de* values of alanine scanning mutants toward **i**, (D) *ee* and *de* values of alanine scanning mutants toward **n**.

Table 3
Relative activity analysis of *Sv*IRED and mutants toward **a, i**, and **n**.

Mutant	Relative activity (%)		
	a	**i**	**n**
WT	100[a]	100[b]	100[c]
L180A	65.2 ± 1.2	34.9 ± 3.2	9.7 ± 0.5
M19A	112.6 ± 5.8	96.5 ± 2.3	136.4 ± 1.2
M125A	194.1 ± 7.4	93.4 ± 3.2	128.5 ± 3.7
D246A	203.3 ± 3.53	110.0 ± 0.2	442.1 ± 6.7
L179A	104.8 ± 7.4	98.6 ± 1.0	54.7 ± 8.3
I124A	101.1 ± 4.0	103.4 ± 2.7	200.2 ± 3.9
P128A	52.6 ± 5.0	48.5 ± 3.4	118.4 ± 6.4
V137A	48.9 ± 4.4	72.8 ± 7.6	28.5 ± 3.5
M183A	88.9 ± 5.7	86.9 ± 3.2	206.8 ± 4.5
I127A	47.5 ± 3.9	34.9 ± 4.3	30.7 ± 2.7
M214A	37.6 ± 3.1	17.7 ± 2.5	47.9 ± 3.5
I218A	58.4 ± 4.4	66.9 ± 2.3	187.8 ± 5.7
V217A	15.1 ± 3.2	30.6 ± 1.3	28.6 ± 0.4
H244A	22.7 ± 6.4	13.8 ± 4.2	120.9 ± 2.2
D238A	22.5 ± 3.4	12.1 ± 3.0	153.1 ± 4.2
V243A	13.1 ± 3.5	11.6 ± 5.5	80.8 ± 2.6

Note:.
[a] 100 %: 17.3 mU/mg.
[b] 100 %: 1.5 mU/mg.
[c] 100 %: 0.3 mU/mg.

forming an alkyl interaction with V243 and coenzyme (Fig. 4**C**), which was similar as M183A. Besides, there was also alkyl interaction between the side chain of M183 and the cyclic group of substrate. However, in H244A, conformation of **1** was different to WT because of the existence of diverse interactions, leading to different selectivity of H244A. The orientation of ester group of **1** was fixed by alkyl interaction between side chains of M214, M125, and hydrogen-bond interaction between M125 and oxygen atom of the ester group. Extra interactions including alkyl interaction between A239 and the cyclic ring, and hydrogen-bond between I124 and the hydrogen atom of pyrrolidine (Fig. 4**D**) were observed in H244A, which was consistent with its higher activity.

4. Conclusion

In summary, a novel imine reductase *Sv*IRED was identified from *Streptomyces viridochromogenes* by gene mining displaying high activity and selectivity in the dynamic kinetic reductive amination of cyclic *β*-ketoester. Enzyme characterization revealed the optimum pH and temperature were 7.0 and 30 °C. Various amine donors could be utilized by *Sv*IRED to produce chiral *N*-substituted *β*-amino esters with different diastereoselectivity and enantioselectivity. The enantioselectivity of *Sv*IRED toward methylamine and pyrrolidine were opposite with *ee* values of 21 % (1*S*, 2*R*) and 79 % (1*S*, 2*R*) Molecular docking and alanine scanning were performed to identify M183A with inverted *ee* value of >99 % (1*R*, 2*S*) and *de* value of >99 % (*cis:trans*) towards methylamine, and H244A with inverted *ee* value of 88 % (1*R*, 2*S*) and *de* value of >99 % (*cis:trans*) towards pyrrolidine. Interaction analysis revealed that the orientation of the ester group played a crucial role in controlling the selectivity of *Sv*IRED. This study provides stereoselective imine reductase for the synthesis of chiral *N*-substituted β-amino esters and useful guidance for protein engineering the preference of amine donors.

Availability of data and materials

The data involved in this study are all included in the article and the supplementary material.

Funding

We are grateful to the National Key R&D Program (2019YFA0906401), National Natural Science Foundation of China (22078127) for the financial support of this research, Postgraduate Research & Practice Innovation Program of Jiangsu Province (KYCX23_2566), the Fundamental Research Funds for the Central Universities.

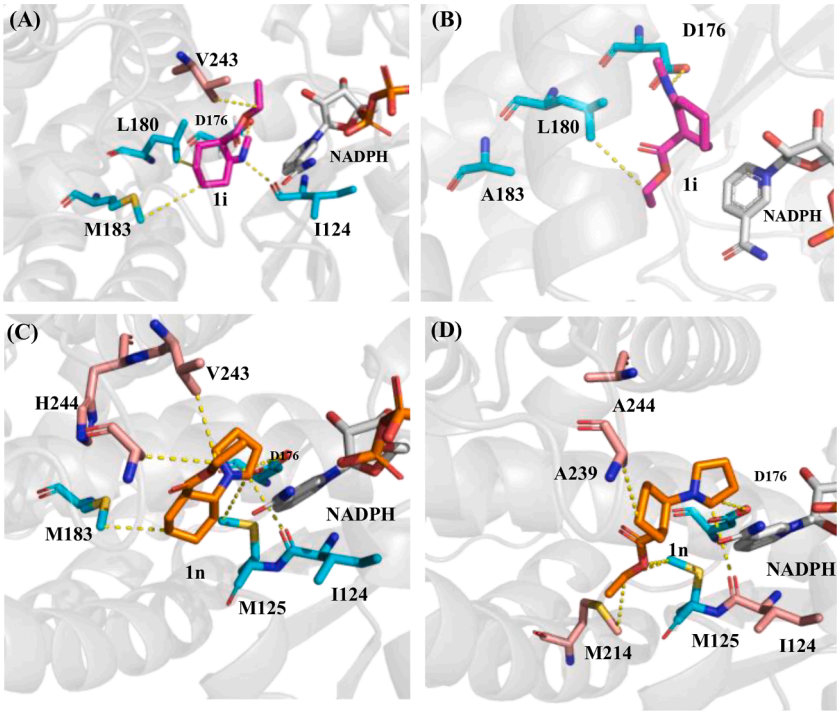

Fig. 4. Interaction analysis of **1i**, and **1n** with residues in the active center of WT *Sv*IRED, M183A, and H244A. (A) WT-**1i**, (B) M183A-**1i**, (C) WT-**1n**, (D) H244A-**1n**.

Ethical statement

The study in this paper does not involve any study of the human rights and ethnic situation.

Supplementary material associated with this article can be found in the online version, at doi:.

CRediT authorship contribution statement

Xiangyu Zheng: Formal analysis, Data curation, Investigation, Methodology, Writing – original draft. **Zhe Dou:** Data curation, Investigation, Methodology. **Wenqiang Xiang:** Data curation, Methodology. **Wen Zhang:** Data curation, Validation. **Ye Ni:** Funding acquisition, Supervision, Resources, Writing – review & editing. **Guochao Xu:** Conceptualization, Funding acquisition, Supervision, Resources, Writing – review & editing.

Declaration of competing interest

The authors declare that they have no known competing financial interests or personal relationships that could have appeared to influence the work reported in this paper.

Data availability

Data will be made available on request.

Supplementary materials

Supplementary material associated with this article can be found, in the online version, at doi:10.1016/j.mcat.2024.114039.

References

[1] B. Yuan, D.M. Yang, G. Qu, N.J. Turner, Z.T. Sun, Biocatalytic reductive aminations with nad(p)h-dependent enzymes: enzyme discovery, engineering and synthetic applications, Chem. Soc. Rev. 53 (2024) 227–262, https://doi.org/10.1039/d3cs00391d.

[2] E.E. Ferrandi, D. Monti, Amine transaminases in chiral amines synthesis: recent advances and challenges, World J. Microbiol. Biotechnol. 34 (2018) 10, https://doi.org/10.1007/s11274-017-2395-2.

[3] J. Wencel-Delord, T. Dröge, F. Liu, F. Glorius, Towards mild metal-catalyzed c-h bond activation, Chem. Soc. Rev. 40 (2011) 4740–4761, https://doi.org/10.1039/c1cs15083a.

[4] S. Liu, Z.F. Wang, K. Chen, L.L. Yu, Q.H. Shi, X.Y. Dong, Y. Sun, Cascade chiral amine synthesis catalyzed by site-specifically co-immobilized alcohol and amine dehydrogenases, Catal. Sci. Technol. 12 (2022) 4486–4497, https://doi.org/10.1039/d2cy00514j.

[5] T.C. Nugent, M. El-Shazly, Chiral amine synthesis - recent developments and trends for enamide reduction, reductive amination, and imine reduction, Adv. Synth. Catal. 352 (2010) 753–819, https://doi.org/10.1002/adsc.200900719.

[6] J. Yamaguchi, A.D. Yamaguchi, K. Itami, C.H. bond functionalization, Emerging synthetic tools for natural products and pharmaceuticals, Angew. Chem. Int. Ed. 51 (2012) 8960–9009, https://doi.org/10.1002/anie.201201666.

[7] T. Hayashi, M. Kawai, N. Tokunaga, Asymmetric synthesis of diarylmethyl amines by rhodium-catalyzed asymmetric addition of aryl titanium reagents to imines, Angew. Chem. Int. Ed. 43 (2004) 6125–6128, https://doi.org/10.1002/anie.200461338.

[8] U.T. Bornscheuer, G.W. Huisman, R.J. Kazlauskas, S. Lutz, J.C. Moore, K. Robins, Engineering the third wave of biocatalysis, Nature 485 (2012) 185–194, https://doi.org/10.1038/nature11117.

[9] P.N. Devine, R.M. Howard, R. Kumar, M.P. Thompson, M.D. Truppo, N.J. Turner, Extending the application of biocatalysis to meet the challenges of drug development, Nat. Rev. Chem. 2 (2018) 409–421, https://doi.org/10.1038/s41570-018-0055-1.

[10] F. Belov, A. Mildner, T. Knaus, F.G. Mutti, J. von Langermann, Crystallization-based downstream processing of ω-transaminase- and amine dehydrogenase-catalyzed reactions, React. Chem. Eng. 8 (2023) 1427–1439, https://doi.org/10.1039/d2re00496h.

[11] I. Slabu, J.L. Galman, R.C. Lloyd, N.J. Turner, Discovery, engineering, and synthetic application of transaminase biocatalysts, ACS Catal. 7 (2017) 8263–8284, https://doi.org/10.1021/acscatal.7b02686.

[12] M.J. Abrahamson, J.W. Wong, A.S. Bommarius, The evolution of an amine dehydrogenase biocatalyst for the asymmetric production of chiral amines, Adv. Synth. Catal. 355 (2013) 1780–1786, https://doi.org/10.1002/adsc.201201030.

[13] H. Ming, B. Yuan, G. Qu, Z.T. Sun, Engineering the activity of amine dehydrogenase in the asymmetric reductive amination of hydroxyl ketones, Catal. Sci. Technol. 12 (2022) 5952–5960, https://doi.org/10.1039/d2cy00391k.

[14] G. Grogan, Synthesis of chiral amines using redox biocatalysis, Curr. Opin. Chem. Biol. 43 (2018) 15–22, https://doi.org/10.1016/j.cbpa.2017.09.008.

[15] A.K. Gilio, T.W. Thorpe, N. Turner, G. Grogan, Reductive aminations by imine reductases: from milligrams to tons, Chem. Sci. 13 (2022) 4697–4713, https://doi.org/10.1039/d2sc00124a.

[16] R. Kumar, M.J. Karmilowicz, D. Burke, M.P. Burns, L.A. Clark, C.G. Connor, E. Cordi, N.M. Do, K.M. Doyle, S. Hoagland;, et al., Biocatalytic reductive

amination from discovery to commercial manufacturing applied to abrocitinib JAK1 inhibitor, Nat. Catal. 4 (2021) 775–782, https://doi.org/10.1038/s41929-021-00671-5.
[17] J.R. Marshall, P. Yao, S.L. Montgomery, J.D. Finnigan, T.W. Thorpe, R.B. Palmer, J. Mangas-Sanchez, R.A.M. Duncan, R.S. Heath, K.M. Graham;, et al., Screening and characterization of a diverse panel of metagenomic imine reductases for biocatalytic reductive amination, Nat. Chem. 13 (2020) 140–148, https://doi.org/10.1038/s41557-020-00606-w.
[18] J.H. Schrittwieser, S. Velikogne, W. Kroutil, Biocatalytic imine reduction and reductive amination of ketones, Adv. Synth. Catal. 357 (2015) 1655–1685, https://doi.org/10.1002/adsc.201500213.
[19] N. Hermanns, S. Dahmen, C. Bolm, S. Bräse, Asymmetric, catalytic phenyl transfer to imines: highly enantioselective synthesis of diarylmethylamines, Angew. Chem. Int. Ed. 41 (2002) 3692–3694, https://doi.org/10.1002/1521-3773(20021004)41:19≤3692::Aid-anie3692≥3.0.Co;2-n.
[20] D. Wetzl, M. Gand, A. Ross, H. Müller, P. Matzel, S.P. Hanlon, M. Müller, B. Wirz, M. Höhne, H. Iding, Asymmetric reductive amination of ketones catalyzed by imine reductases, ChemCatChem 8 (2016) 2023–2026, https://doi.org/10.1002/cctc.201600384.
[21] G.A. Aleku, S.P. France, H. Man, J. Mangas-Sanchez, S.L. Montgomery, M. Sharma, F. Leipold, S. Hussain, G. Grogan, N.J. Turner, A reductive aminase from *Aspergillus oryzae*, Nat. Chem. 9 (2017) 961–969, https://doi.org/10.1038/nchem.2782.
[22] P. Yao, J.R. Marshall, Z. Xu, J. Lim, S.J. Charnock, D. Zhu, N.J. Turner, Asymmetric synthesis of n -substituted α-amino esters from α-ketoesters via imine reductase-catalyzed reductive amination, Angew. Chem. Int. Ed. 60 (2021) 8717–8721, https://doi.org/10.1002/anie.202016589.
[23] J. Zhang, D. Liao, R. Chen, F. Zhu, Y. Ma, L. Gao, G. Qu, C. Cui, Z. Sun, X. Lei;, et al., Tuning an imine reductase for the asymmetric synthesis of azacycloalkylamines by concise structure-guided engineering, Angew. Chem. Int. Ed. (2022) 61, https://doi.org/10.1002/anie.202201908.
[24] M. Schober, C. MacDermaid, A.A. Ollis, S. Chang, D. Khan, J. Hosford, J. Latham, L. A.F. Ihnken, M.J.B. Brown, D. Fuerst;, et al., Chiral synthesis of lsd1 inhibitor gsk2879552 enabled by directed evolution of an imine reductase, Nat. Catal. 2 (2019) 909–915, https://doi.org/10.1038/s41929-019-0341-4.
[25] J. Zhang, X. Li, R. Chen, X. Tan, X. Liu, Y. Ma, F. Zhu, C. An, G. Wei, Y. Yao;, et al., Actinomycetes-derived imine reductases with a preference towards bulky amine substrates, Commun. Chem. 5 (2022) 123, https://doi.org/10.1038/s42004-022-00743-y.
[26] K. Murugesan, T. Senthamarai, V.G. Chandrashekhar, K. Natte, P.C.J. Kamer, M. Beller, R.V. Jagadeesh, Catalytic reductive aminations using molecular hydrogen for synthesis of different kinds of amines, Chem. Soc. Rev. 49 (2020) 6273–6328, https://doi.org/10.1039/c9cs00286c.
[27] J. Citoler, V. Harawa, J.R. Marshall, H. Bevinakatti, J.D. Finnigan, S.J. Charnock, N.J. Turner, Synthesis of pharmaceutically relevant 2-aminotetralin and 3-amino-chroman derivatives via enzymatic reductive amination, Angew. Chem. Int. Ed. 60 (2021) 24456–24460, https://doi.org/10.1002/anie.202110321.
[28] F.F. Chen, X.F. He, X.X. Zhu, Z. Zhang, X.Y. Shen, Q. Chen, J.H. Xu, N.J. Turner, G. W. Zheng, Discovery of an imine reductase for reductive amination of carbonyl compounds with sterically challenging amines, J. Am. Chem. Soc. 145 (2023) 4015–4025, https://doi.org/10.1021/jacs.2c11354.
[29] F. Ruebsam, C.V. Tran, L.S. Li, S.H. Kim, A.X. Xiang, Y.F. Zhou, J.K. Blazel, Z. X. Sun, P.S. Dragovich, J.J. Zhao, et al., 5,6-dihydro-1-pyridin-2-ones as potent inhibitors of hcv ns5b polymerase, Bioorg. Med. Chem. Lett. 19 (2009) 451–458, https://doi.org/10.1016/j.bmcl.2008.11.048.
[30] Z. Szakonyi, Á. Csőr, M. Haukka, F. Fülöp, Stereoselective synthesis of carane-based chiral β- and γ-amino acid derivatives via conjugate addition, Tetrahedron 71 (2015) 4846–4852, https://doi.org/10.1016/j.tet.2015.05.019.
[31] E. Iglesias, Ester hydrolysis and enol nitrosation reactions of ethyl cyclohexanone-2-carboxylate inhibited by β-cyclodextrin, J. Org. Chem. 65 (2000) 6583–6594, https://doi.org/10.1021/jo0007231.
[32] D.Q. Xu, K. Prasad, O. Repic, T.J. Blacklock, A practical synthesis of enantiopure ethyl cis-2-amino-1-cyclohexanecarboxylate via asymmetric reductive amination methodology, Tetrahedron-Asymmetry 8 (1997) 1445–1451, https://doi.org/10.1016/s0957-4166(97)00160-2.
[33] M. Sharma, J. Mangas-Sanchez, S.P. France, G.A. Aleku, S.L. Montgomery, J. I. Ramsden, N.J. Turner, G. Grogan, A mechanism for reductive amination catalyzed by fungal reductive aminases, ACS Catal. 8 (2018) 11534–11541, https://doi.org/10.1021/acscatal.8b03491.
[34] M.J. Plevin, D.L. Bryce, J. Boisbouvier, Direct detection of CH/π interactions in proteins, Nat. Chem. 2 (2010) 466–471, https://doi.org/10.1038/nchem.650.
[35] F.A. Perras, D. Marion, J. Boisbouvier, D.L. Bryce, M.J. Plevin, Observation of CH•••π interactions between methyl and carbonyl groups in proteins, Angew. Chem. Int. Ed. 56 (2017) 7564–7567, https://doi.org/10.1002/anie.201702626.